RUSSIAN SPACEBORNE LIDAR "BALKAN "

Yu.S. Balin, I.V. Znamenskii, V.E. Zuev, V.E. Mel'nikov, S.V. Samoilova, and A.A. Tikhomirov

Institute of Atmospheric Optics, Siberian Branch of the Russian Academy of Sciences, Tomsk.
Received January 29, 1995.

The paper presents a description of the first Russian spaseborne single-frequency aerosol lidar. The lidar is designed for investigating clouds and the Earth's surface and is planned to be mounted inside SPEKTR module of the MIR orbiting station. It consists of a transceiver, recording and control systems. Some aspects of the sounding data interpretation are considered.

1. INTRODUCTION

At present the principal source of information about the atmosphere and underlying surface obtained from satellites in the visible spectral range are the photographic and radiometric observations carried out with the passive sounding tools.

The active laser sounding tools (lidars) are not yet widely used for monitoring from space because they are still under technological tests. The first, in the worldwide practice, flight of a spaceborne aerosol lidar onboard a spacecraft launched by NASA early in the fall of 1994 within the framework of the LITE program is an example of such a technological experiment.[1] The Russian–French spaceborne lidar ALISA is being actively prepared.[2]

This paper describes the first Russian spaceborne lidar BALKAN produced in 1989[3] and intended for investigating optical and physical parameters of cloud fields and the Earth's surface, as well as the aforementioned lidars.

When realizing this project, we took into account the necessity of using at maximum the available experience in the spaceborne and ground based measurements. So, in order to shorten the development period and to increase the reliability of the instrumentation, we used many elements of operating spaceborne geodesic laser range finders.

Thus, one of the important decisions concerns the system of data processing onboard the satellite. In the majority of available ground based lidars data are processed immediately after the experiment by means of a computer included into the lidar. Since we did not know the real signal characteristics we have decided to make no data processing onboard a satellite. The signal received is evaluated and the data are transferred to the ground based station through the telemetric channel in the raw form for further analysis.

This allows us to simplify significantly the recording system, to avoid some errors, and to gain the experience for subsequent development.

2. GENERAL DESCRIPTION OF THE LIDAR

By the construction principle used in the BALKAN lidar it is a typical lidar complex consisting of the following blocks: a transceiver, a geodesic channel of range finding, a system for recording the lidar returns, and the control desk.

The lidar is mounted onboard the SPEKTR module, the third module of the manned MIR orbiting station. The transceiver of the lidar is mounted on the bracket in front of an illuminator made of special glass 400 mm in diameter. The detecting block is mounted near the transceiver, and the control desk is at the working place of an astronaut.

Principal specifications of the lidar.

Wavelength, nm	532
Pulse energy, J	0.2
Pulse duration, ns	12
Pulse repetition frequency, Hz	0.18
Transmitting collimator diameter, mm	120
Beam divergence at the output of the laser transmitter, mrad	0.15
Receiving telescope diameter, mm	275
Field of view, mrad	0.44
Transmission FWHM of the interference filter, nm	3
Quantum efficiency of a PMT, %	13
Light power threshold of the receiver, W	$2 \cdot 10^{-8}$
Band width of an amplifier, MHz	40
Error of the range finding, m	0.75
Number of digits of the ADC, bit	6
Time resolution of the ADC, ns	20
Electric power consumption, W	200
Mass, kg	120

To increase the reliability of the instrumentation, as it is accepted in the space technology, the "cold" and "hot" reservation of blocks and elements of the lidar is used.

The "cold" reservation is used for the recording block and the source of radiation. Two photodetector channels operating simultaneously are in the "hot" reservation.

0235-6880/95/09 711-07 $02.00

Figure 1 illustrates the principles of measuring the signals reflected from clouds and the underlying surface. Two recording channels, range finder and lidar, operating simultaneously are used for measurements.

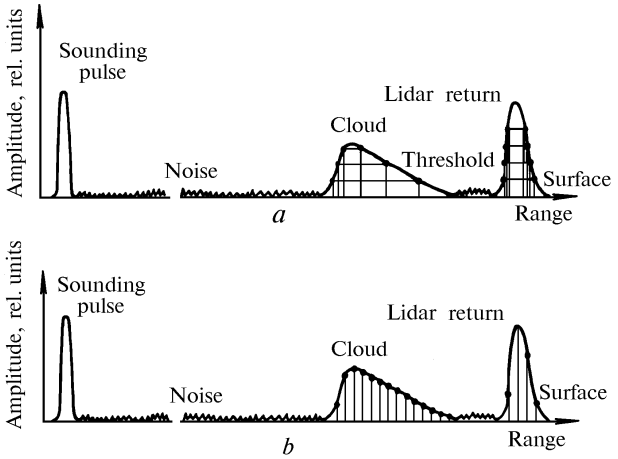

FIG. 1. Technique for recording signals by means of range finder (a) and lidar (b) channels.

The range finder channel is based on four different devices operating when the signal has exceeded the threshold value of $2 \cdot 10^{-8}$ W as measured at the input of a photodetector. Then the time (range) is determined at the moment of exceeding the threshold within the leading and trailing edges of the return signal. Lidar channel uses an ADS for recording the return signal with a 3 m resolution.

The dots on signal envelopes show amplitude sampling points and time intervals being measured using both recording channels.

When using the range finder channel, the cases are possible (Fig. 1 *a*) when the value of a return from a cloud is below the maximum threshold value. Nevertheless, the existence of the range finder channel makes it possible to duplicate the lidar channel records, and, as it will be shown in the second part of the paper, to estimate the optical density of a cloud.

3. TRANSCEIVER

General view of the transceiver of the lidar is shown in Fig. 2. The laser block is shown on its left, and the optical part consisting of the laser collimator and the receiving telescope is on its right.

The transceiver is produced as a unit cast that provides keeping the optical axes of receiving and transmitting systems in parallel with an accuracy not worse than ± 10″. Optical antennas and the laser are fastened to each other, that provides necessary rigidity of the system.

Optical diagram of the transceiver is shown in Fig. 3.

Transmitting antenna consisting of a three–lens objective and a two–lens ocular is the Galilean telescope that provides essential decrease in the laser beam divergence. Antireflection coating of the objectives provides for their transmission to be about 0.87.

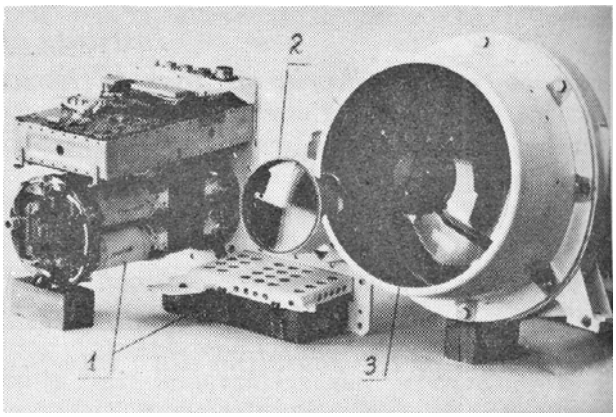

FIG. 2. General view of the transceiver of the BALKAN lidar: 1) lasers, 2) collimator, 3) receiving telescope.

A mirror–lens telescope of the Mangene scheme is used in the receiving optical antenna. External surface of the mirror is coated with a reflecting cover. Such a system allows the significant decrease in the length of the telescope. The screening by the secondary mirror is less than 0.3. Antireflection coatings of the optical components in combination with the reflecting surfaces make the end–to–end transmission of the receiving optics at the wavelength 532 nm to be about 0.7. The field stop is placed in the focal plane. It provides the receiving field of view about 90±5 seconds of an arc. The Fabry lense is used for forming the output pupil of 8 mm diameter. Light beam divergence at its output is not more than 3°.

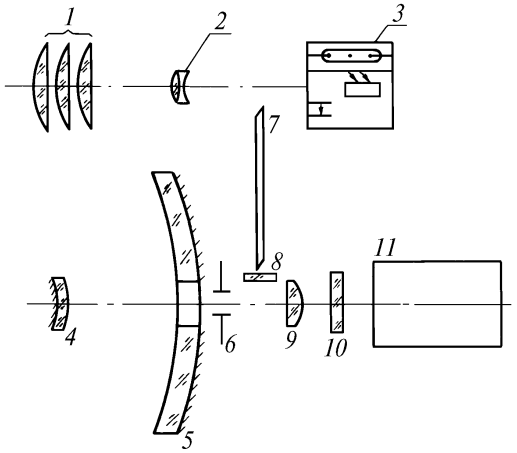

FIG. 3. Optical arrangement of the BALKAN lidar: 1) and 2) collimators, 3) laser, 4) and 5) receiving telescope, 6) field stop, 7) optical waveguide, 8) filter, 9) Fabry lens, 10) interference filer, 11) photodetector.

A portion of the laser beam scattered by the front surface of the ocular *2* is directed to the receiving system through the optical waveguide *7*. The filter *8* of the SZS–23 glass is used for removing the fundamental harmonic of the laser radiation. After the conversion, in the block *11*, into the electrical signal, this portion of laser radiation is used as a triggering pulse in the lidar return processing.

3.1. Laser transmitter

An Nd:YAG laser with frequency doubling is used in the lidar. Two transmitting channels, main and reserved, are used to increase the reliability and resource of the lidar operation. Superposition of beam axes of the main and reserved sources is performed with the commutation and beam folding prisms. The sources are switched automatically at the absence of two consequitive pulses or under the command from the control unit.

The main and reserved channels are identical. Each of them includes a master oscillator, two single–path amplifiers, and frequency doubler. Optical diagram of one of the sources is shown in Fig. 4.

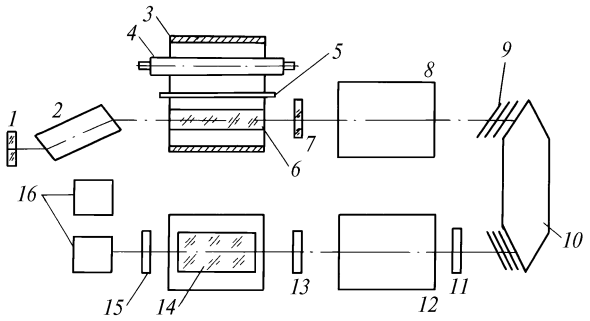

FIG. 4. Optical arrangement of the laser source: 1) 100% reflecting mirror, 2) electrooptical Q–switch, 3) reflector, 4) pumping flash lamp, 5) filter, 6) active element, 7) sapphire plate, 8) and 12) optical amplifiers, 9) plates, 10) beam folding prism, 11) and 13) optical quater–wave plates, 14) frequency doubler, 15) filter, 16) radiation convergence prisms.

The master oscillator includes resonator, optical Q–switch, and an active element inside a cavity. The resonator is formed by the mirror with the reflection coefficient of 100% and the sapphire plate with the reflection coefficient of 16%.

The active element is an Nd:YAG crystal of cylindrical shape with the size 6.3×65 mm. The filter cutting out the UV radiation of the flash lamp radiation spectrum is used in the cavity. The amplifiers differ from the master oscillator only by the absence of a resonator and a Q–switch. The frequency doubler converts the IR radiation with the power of order 0.5 J passing through it into visible one with the conversion efficiency of 50%. A nonlinear element, CDA crystal of 10×10×40 mm size, is used. It is placed into a thermostat that keeps the temperature with an accuracy of 0.1 K. The quater–wave plates *11* and *13* together with the plane plates *9* placed at the Brewster angle serve for suppressing the free generation in the laser. The filter *15* cuts the fundamental harmonic of the laser, and the beam folding prism *10* is used to shorten the laser length. The convergence prism *16* is capable of directing the output radiation along the optical axis of the laser output pupil. The close packing of the laser block and the absence of water cooling limit the pulse repetition frequency by the value of 5.6 s. Then the pulse number in a single series of shots cannot exceed 80, with the interruption between series of 30 min.

3.2. Photodetecting block

Block diagram of the photodetecting block of the lidar is shown in Fig. 5. The basis of the optical detector is a PMT FEU–84 that has a good quantum efficiency in the visible range. To increase the reliability of the lidar return recording, two photomultipliers operate simultaneously in the photodetecting block. To increase the efficiency of detecting the light flux, the total internal reflection prisms are placed on their butt–ends. The interference filter is fastened immediately on the photodetecting block body by means of a special wedge providing the filter transmittance at the wavelength of 532 nm. After photoelectrical conversion, the signals are amplified and directed to the summing formers. For a higher reliability, the signals from both photomultipliers are summed up.

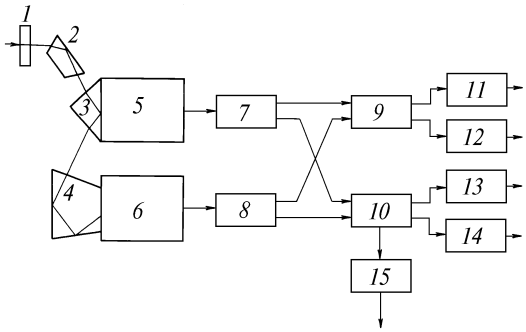

FIG. 5. Block diagram of the photodetecting block: 1) interference filter, 2) beam folding prism, 3) and 4) total internal reflection prisms, 5) and 6) PMTs, 7) and 8) amplifiers, 9) and 10) summing devices, 11) – 14) threshold devices, 15) emitter follower.

The nonlinear digital filtration of signals based on selection of the reflecting pulse duration is used in the range finder channel of the recording system. Two threshold devices with different light power threshold are placed at the output of each summing device. The minimum threshold is $2 \cdot 10^{-8}$ W. Then the signals are fed from the threshold devices to the channel of determining the distance from the object for processing.

Simultaneously, the signal is directed from the output of the summing device through the emitter follower to the ADC of the signal recording channel. This channel has two modes of operation, the "day" and "night" ones.

The photodetector amplification coefficient in the "night" regime increases relative to the "day" regime by 15 Db by increasing the photomultiplier voltage. Finally, it will allow us to investigate the lidar system sensitivity when sounding different objects including the case of variable background component of the signal.

4. RECORDING SYSTEM OF THE LIDAR

As was mentioned above, the system for recording the lidar returns consists of two independent channels, the range finder (amplitude–distance) and lidar (distance–amplitude).

The range finder channel provides the determination of the distance from the sounded object by measuring the time interval between the sounding pulse and the reflected signal exceeding the threshold value. Since the signal reaches the threshold at its leading and trailing edges, one can also determine its duration at different amplitude levels (Fig. 1). In an ideal case, when the return signal value exceeds the maximum threshold, a complex is formed of four pairs of amplitude and distance values and one can estimate optical parameters of clouds by analyzing them.

This information is transformed in a special processor of the channel into the binary digital code corresponding to the exact value of the distance from the object.

The lidar recording system is based on measurement of signal amplitudes at fixed time moments counted from the moment of the pulse emission. The six–digit ADC with sampling time of 20 ns is used for this purpose. Amplitude sample of a signal is recorded into a RAM where the data on the shot passport are fixed simultaneously. This data have the form of 22–bit binary code of the time of sounding (day, hour, minutes, seconds) and the 18–bit code of the sounding cycle number. In addition, the shot passport contains the data on the distance from the object. All this data are formed in RAM in a single information string of 31 byte length whose structure is shown in Fig. 6.

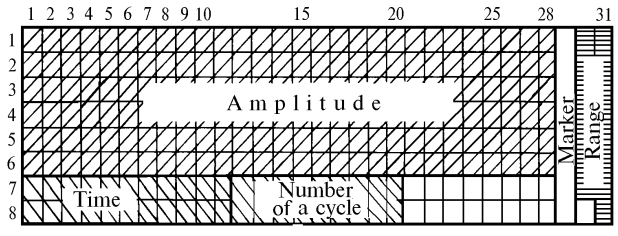

FIG. 6. Information string format.

If the lidar signal duration has exceeded 560 ns, the information on the signal residue is recorded in the next information string with the same passport data. After recording 8 information strings, the RAM content is automatically stored in the buffer memory device (BMD). Thus compiled information is then transferred from BMD to the telemetric system of the MIR station on command from the onboard computer complex.

The scientific and service telemetric data are decoded and processed in the Flight Controlling Center.

5. CONTROL DESK AND GROUND BASED INSTRUMENTATION COMPLEX

The control desk provides the control of operation of all lidar parts, including the automated account of the measurement cycle numbers. In addition, it provides receiving and distributing the control commands from the onboard systems of the orbiting station.

Control of the lidar is semi–automated, and the choice of the regime of operation is determined by an austronaut–operator depending on the purposes of the space experiment conducted. Sounding can be carried out with both a single shot and shot series. In addition, the provision is made for its installation onboard an unmanned satellite.

After switching on the instrumentation, heating of the thermostat blocks of the lidar and self–control of their operation take 40 min. This service information comes to the indicators of the control desk, and is transferred to the Flight Controlling Center via telemetric system.

After finishing of the sounding cycle, the lidar blocks are switched off. The voltage release from the signal recording system is blocked until the finish of data transfer into the telemetric complex of the station.

Ground based instrumentation complex is indended for performing the control and test measurements of electrical and optical parameters of the lidar for operation in autonomous regime and in the instrumentation complex of the MIR station. The complex includes electrical and optical imitators of lidar signals, optical instrumentation for alignment and testing of the transceiver, and instrumentation for testing the electrical parameters of the lidar and its parts.

The climatic, mechanical and acoustical tests of the lidar, including the tests for the effect of electromagnetic interferences, were carried out using this complex.

The size–mass, technological, and training prototypes of the BALKAN lidar were produced for these purposes.

6. SOUNDING DATA INTERPRETATION

The model calculations of the power of lidar returns from clouds of different types were carried out for the aforementioned lidar parameters. As the model estimates show, the lidar signal power is mainly determined by two cloud parameters, the scattering coefficient and its vertical gradient at the upper boundary of the cloud. So the returns from clouds with small optical gradient can be less than the lidar sensitivity threshold thus being undetectable by its recording system.

Another problem that should be considered, when creating the processing algorithms, is few number of the signal amplitude readouts due to the specific features of measurements.

6.1. Signal processing technique

When creating the algorithm for processing of lidar returns, the analysis has been carried out of the experimental data on locating underlying surface and cloud fields using the range finder channel, i.e. when recording the signal in the threshold regime.

A portion of these data represented in the form of returns from clouds, water and steppe surface are shown in Fig. 7. The x–axis in it is the distance corresponding to the moments at which signal reaches the first threshold level at its leading and trailing edges. The y–axis is the threshold power in relative units.

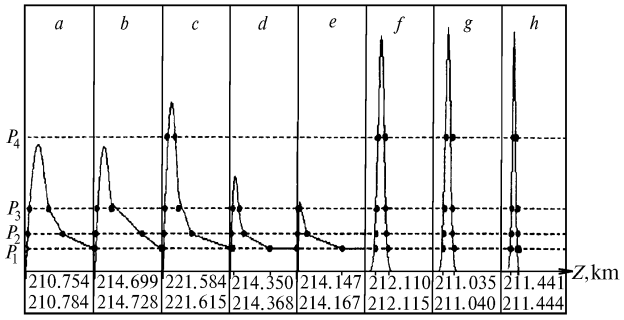

FIG. 7. Lidar signal profiles from clouds (a–c), water (d–e) and steppe (f–h) surfaces. Dots on the curves show the signal amplitude received by the range finder channel.

As is seen from the figure, the signal from clouds and underlying surface (steppe) are different in both shape and intensity. Water surface is an intermediate case between them. It is revealed from the analysis of all data that in the majority of events (90%) signals from clouds do not reach the fourth maximum threshold, and their duration at the minimum level is 15–30 m. For the 3 m spatial resolution realized in the lidar it can lead to few number of readouts thus imposing specific requirements on the processing algorithms. Total procedure of the lidar signal processing includes three sequential stages. The first is filtration, i.e. discrimination of the signal against the interference background and removing the instrumental errors. The second is classification, i.e. recognizing the kind of sounded object (cloud or underlying surface). The third stage is the processing of lidar signal for estimation of optical and physical parameters of clouds and underlying surfaces.

Filtration. This stage of the lidar signal processing is the most universal, requires minimum *a priori* information on the physical state of the object and can be easily automated. Its necessity is caused by the desire, first, to decrease the effect of random interferences of background and instrumentation origin, second, to remove the instrumental distortions of the lidar signal due to its broadening. The matter is that the lidar signal has a short duration due to specific conditions of the experiment, especially, when sounding the underlying surface comparable with the pulse duration. At the same time, because of a limited bandwidth of the receiving channel, it leads to a decrease in the lidar signal and distorting its time structure.

This fact can be illustrated by the data from Table I where the variation of the lidar signal duration shown in Fig. 7 is presented.

TABLE I. Influence of the limitation of the electronic bandwidth of the receiving path on the duration of lidar signals.

Signal	d, mm	d_0, km	d/d_0
a	0.008625	0.008517	1.01
b	0.008625	0.008176	1.05
c	0.005625	0.005298	1.06
d	0.004125	0.003542	1.16
e	0.006000	0.004240	1.41
f	0.003375	0.002718	1.24
g	0.002625	0.001903	1.38
h	0.001875	0.000999	1.88

The parameter d_0 in Table I corresponds to the reconstructed signal duration (at the level $P = P_2$) for the bandwidth of 10 MHz and sounding pulse duration of 10 ns. Reconstruction was done using the inverse filtration algorithms.[4]

Classification. This stage is necessary because interpretation of the spaceborne lidar data without involving some *a priori* information can be ambiguous. There is a probability of the false decision on the kind of the scattering object due to a highly variable nature of the "atmosphere–underlying surface" system.

To construct the classification algorithms, it is necessary to select the minimum bulk of essential information parameters of a signal and to provide their maximum independence. Many signal parameters, such as the rise time, duration, maximum amplitude, etc., are mutually related. As it has been shown in Ref. 5, to provide the classification, one should take the following

characteristics: distance from the sounded object z_0, rise time Δz, and its integral value. The latter value is proportional to the reflection coefficient of the surface or to the backscattering phase function of a cloud. These characteristics contain almost all information about the object sounded that can be obtained at single–frequency sounding, when analyzing energetic parameters of the return signal.

Estimation of the parameters. The selected characteristics can give an information about the physical state of the object under investigation, so their separate values are of independent interest. In particular, the cloud upper boundary is determined from the distance, and then some geodesic problems can be solved. The integral value of the signal characterizes the optical state of the object. The third parameter, rise time, depends on the behavior of the scattering coefficient at the cloud upper boundary.

Assuming that the parameter $\sigma(z)$ increases linearly, the third parameter is unambiguously related to the gradient:

$$\frac{d\sigma}{dz} = \frac{1}{2\,\Delta z^2} = \ln\left(\frac{z_2 - z_0}{z_1 - z_0}\right)[(z_2 - z_0)^2 - (z_1 - z_0)^2]^{-1}. \quad (1)$$

The stable estimate of the gradient can be obtained by the least squares method

$$\frac{\hat{d}\sigma}{dz} = \int_{z_1}^{z_2} \ln\frac{(z - z_0)S(z_m)}{(z_m - z_0)S(z)}[(z - z_0)^2 - (z_m - z_0)^2]\,dz \times$$

$$\times\left\{\int_{z_1}^{z_2}[(z - z_0)^2 - (z_m - z_0)^2]^2\,dz\right\}^{-1}. \quad (2)$$

Here $S(z_m)$ is the maximum signal amplitude at the distance z_m; z_1 and z_2 are the distances where the equal amplitude levels are detected within the leading and trailing edges, respectively.

Using these equations, one can estimate z_0, what is worth doing under high noise. As model calculations show, the greatest error in reconstruction is observed when using the trailing edge of a signal. Taking into account that this part of the lidar signal is the most distorted due to the multiple scattering effect, we recommend to use the leading edge of the pulse for sounding data interpretation.

The created algorithms for estimating optical parameters were tested in processing of real signals (Fig. 7)

Calculation results are given in Table II, that shows the distance from cloud z_0, mean values $\bar{\sigma}$, and corresponding values of the optical depth $\tau(z_i)$ for three distances z_i. The distances z_1 and z_2 correspond to the time moment when the signal reaches the maximum threshold (P_3 for (*a*) and (*b*), and P_4 for (*c*)). The distance z_3 corresponds to the penetration of radiation into the cloud to the optical depth $\tau \sim 0.4$.

TABLE II. Results of signal processing.

Parameter	Signal		
	a	*b*	*c*
z_0, km	210.7539	214.6991	221.5641
$z_1 - z_0$, km	0.0016	0.0007	0.0015
$\bar{\sigma}(z_1)$, km^{-1}	19.29	19.02	42.34
$\tau(z_1)$	0.0325	0.0143	0.0648
$z_3 - z_0$, km	0.0065	0.0049	0.0042
$\bar{\sigma}(z_3)$, km^{-1}	64.30	88.73	100.38
$\tau(z_3)$	0.422	0.432	0.417
$z_2 - z_0$, km	0.0099	0.0071	0.0049
$\bar{\sigma}(z_3)$, km^{-1}	95.54	126.77	116.99
$\tau(z_3)$	0.949	0.903	0.574

As is seen from Table II, the results obtained using the information about the pulse trailing edge have the least likelihood, as was noted above.

At the same time, the mean values $\bar{\sigma}$ are in satisfactory agreement with the experimental data on the dense clouds.[6] The values $\bar{\sigma}$ obtained can be used for reconstructing the profile of scattering coefficient by means the algorithms available.[7]

6.2. Numerical experiment

To study the information capacity of laser sounding of the objects from space, the closed numerical experiment was carried out by the statistical test technique. The series of random realizations of the medium parameters were simulated. Then the corresponding realizations of lidar signals were calculated, and then the information parameters were calculated and the classification was carried out. The Bayes classificator was used. Distributions of the main parameters were set to be normal and corresponding to the mean reflection coefficient of 0.1 for water, 0.2 for cloud, and 0.5 for ice. Homogeneous model of the water thickness was used as well as the stratus cloudiness model with 0.5 km mean thickness.[6] The mean value of the distance from the sounded object was equal to 300 km with the rms error of 300 m (for water and ice) and 295 km with rms error of 5 km (for cloud). Variation coefficients of the other parameters was assumed to be equal to 50%. An *a priori* probability of the hypothesis were assumed to be equal to each other.

The errors in distinguishing among the ice, cloud and water surface are given in Table III in per cent when using the following information parameters:

a) only the reflection coefficient (that approximately corresponds to recognizing by the brightness in pictures taken from space when the Sun is at zenith);

b) reflection coefficient and the duration of the leading edge of the reflected pulse;

c) the above parameters and the distance from the sounded object.

As is seen from the Table III, the use of a lidar with the inherently three–dimensional data, makes it possible to increase significantly the reliability of recognizing the kind of natural formations by selecting the objects according to the distance. Together with the available radiometric passive methods, this essentially extends the capabilities of modern radiation measurements.

TABLE III. Errors in recognizing the formation from the sounding data.

Kind of the object	Informative parameters		
	a	*b*	*c*
Ice	32	1	1
Water	45	31	21
Cloud	73	33	3

ACKNOWLEDGMENTS

The BALKAN lidar described in this paper is the product of the joint activity of four organizations: Institute of Atmospheric Optics SB RAS; Design and Technological Institute "Optika", Institute of Space Technology, and Russian Space Center "Energia". We would like to thank all specialists of these organizations who took part in the work on this project.

In addition we should like to thank especially I.V. Samokhvalov, V.V. Burkov, V.S. Il'ichevskii, V.S. Shamanaev, V.I. Efimkin, and Yu.N. Grachyov who took an active part in the development of the lidar presented in this paper.

REFERENCES

1. M.P. McCormic, D.M. Winker, E.V. Browell et al., Bulletin American Meteorol. Soc. **74**, No. 2, 205–214 (1993).
2. *International Complex Project "Priroda". Scientific Program of Experiment* (Radioelectronic Institute Publishing House, Moscow, 1993), 62 pp.
3. Yu.S. Balin, V.V. Burkov, I.V. Znamenskii, et al., *Abstracts of Reports at 15th Int. Las. Radar Conf.*, Tomsk (1990), Vol. 1, pp. 12–14.
4. S.I. Kavkyanov and S.V. Strepetova, Opt. Atm. **1**, No. 6, 50–56 (1988)
5. Yu.S. Balin, S.I. Kavkyanov, G.M. Krekov, et. al., Opt. Atm. **1**, No 1, 93–99 (1988).
6. E.M. Feigelson, ed., *Radiation in the Cloudy Atmosphere* (Gidrometeoizdat, Leningrad, 1981), 280 pp.
7. G.M. Krekov, S.I. Kavkyanov, and M.M. Krekova, *Interpretation of Signals of Optical Sounding of the Atmosphere* (Nauka, Novosibirsk, 1987), 186 pp.